Estimating induced-activation of SCT barrel-modules

C. Buttar, I. Dawson, A. Moraes

Department of Physics and Astronomy, University of Sheffield,
Hicks Building, Hounsfield Road, Sheffield, S3 7RH, UK

c.m.buttar@sheffield.ac.uk, Ian.Dawson@cern.ch, a.m.moraes@sheffield.ac.uk

Abstract

Operating detector systems in the harsh radiation environment of the ATLAS inner-detector will result in the production of radionuclides. This paper presents the findings of a study in which the radioactivation of SCT barrel modules has been investigated.

I. INTRODUCTION

One of the consequences of operating detector systems in the harsh radiation environments of the ATLAS inner-detector [1] will be the radioactivation of the components. If the levels of radioactivity and corresponding dose rates are significant, then there will be implications for any access or maintenance operations. In addition, maintenance operations may be required on nearby detector or machine elements, for example beam-line equipment, so the impact of the SCT has to be considered. A further motivation for understanding SCT activation concerns the eventual storage or disposal of the SCT-modules at the end of the detector lifetime, in which any radioactive material will have to be classified.

Radionuclides are produced in the SCT modules via the inelastic interactions of hadrons with the various target nuclei comprising the modules. The hadrons originate from: 1) secondaries from the p-p collisions, dominated by pions, and 2) backsplash from hadron cascades in the calorimeters, mainly neutrons. Therefore, the calculation of radionuclide production requires a detailed inventory of the target-nuclei comprising the SCT modules and a good knowledge of the corresponding radiation backgrounds.

II. MODULE DESCRIPTION AND MATERIAL INVENTORY

In order to make activation estimates, it is necessary to obtain a detailed inventory of the materials involved in the construction of a module. The relevant information is now becoming available as SCT modules go into the production phase [2]. Of particular importance is knowledge of elements containing isotopes with high neutron capture cross sections. For example, ^{197}Au has a thermal neutron capture cross section ~ 100 b for the (n,γ) process and even small quantities of such an isotope can contribute considerably, or even dominate the activated environment.

In the SCT barrel system there are 4 layers of cylinders, comprising 32, 40, 48 and 56 rows of 12 modules respectively. Each SCT barrel module comprises silicon sensors, baseboard with BeO facings, ASICs and a Cu/polymide hybrid [3], connected to opto-packages and dog-legs [4]. Each row of modules has associated with it a cooling pipe [5] and power tape. In total, the module mass is calculated to weigh 34.6 g and contain 15 different elements. Details of the elemental breakdown are given in Table 1.

Unfortunately, material details are not always given in their elemental form and sometimes have to be derived. Assumptions are therefore unavoidable and include: 1) Thermal adhesives assumed to be 70% polyimide and 30% BN; 2) Epoxy films, polyimide layers with adhesives and PEEK are chemically described as $C_{22}H_{10}N_2O_5$; 3) The solder composition is assumed to be 59% Pb, 40% Sn and 1%Ag; 4) Capacitors made of AlO and resistors 20% C and 80% AlO. Perhaps the most important assumption concerns the possible use of silver loaded conductive glues. Silver is important due to the high thermal neutron capture cross section and long half-life of ^{110m}Ag. In the current study no silver has been assumed in the glues.

III. RADIONUCLIDE PRODUCTION

Radionuclides are produced in the SCT modules via the inelastic interactions of hadrons with the various target nuclei comprising the modules. However, radionuclides with short half-lifes can be neglected as access to the irradiated SCT material is unlikely for at least several days. In the current study, radionuclides are only considered of radiological interest if they have half-lifes greater than 1 hour and less than 30 years.

Radionuclide production can be divided into two categories:

Table 1: Table of barrel module element masses.

Elements	Silicon sensors	Baseboard with BeO facings	ASIC's	Hybrid	Cooling pipe with coolant	Power tape	Opto Package / Dog Leg	Total (g)
H	0.001	0.008	0.004	0.034	-	0.012	0.035	0.094
Be	-	0.597	-	-	-	-	-	0.597
B	0.010	0.054	0.027	0.185	-	-	-	0.276
C	0.037	4.672	0.099	3.024	0.821	0.306	0.926	9.885
N	0.017	0.092	0.045	0.311	-	0.032	0.324	0.821
O	0.011	1.119	0.037	0.442	-	0.093	0.304	2.006
F	-	-	-	-	3.462	-	-	3.462
Al	-	0.118	0.028	0.393	1.166	0.78	0.434	2.919
Si	10.812	-	0.742	0.187	-	-	0.029	11.770
Ni	-	-	-	0.025	-	-	0.015	0.040
Cu	-	-	-	1.501	-	-	1.071	2.572
Ag	-	-	-	0.001	-	-	0.0004	0.0014
Sn	-	-	-	0.049	-	-	0.012	0.061
Au	-	-	-	0.011	-	-	-	0.011
Pb	-	-	-	0.073	-	-	0.024	0.097
Total (g)	10.888	6.660	0.982	6.236	5.449	1.223	3.174	34.612

1. Production via low energy ($<$ 20MeV) neutron interactions, eg (n,γ), (n,p), (n,α), (n,np) etc.. The cross sections for these neutron interactions are well known for the target nuclei being considered [6]. The production probability for each radionuclide of interest, per target nuclei, can be obtained by convolving the energy dependent cross sections with neutron energy spectra. The radiation environment of the SCT environment has previously been studied [1] and neutron energy spectra obtained. According to these studies, thermal neutrons account for more than a half of the total neutron fluences in and around the SCT barrel system. In the current study, the radionuclide production probabilities were evaluated for all the low-energy neutron interactions and, as expected, the dominant process was found to be thermal-neutron capture (n,γ).

   Values of radionuclide production per p-p event per module from (n,γ) interactions are obtained simply from $n\,\phi\,\sigma$ where n is the number of atoms of a given isotope in the module and σ is the corresponding thermal neutron cross section, obtained from [7]; ϕ is the thermal neutron fluence which, according to [1], has the value 2×10^6 n cm^{-2} s^{-1} over the whole SCT barrel system. It should be noted, however, that the inner detector thermal neutron rates are likely to be smaller in reality than those predicted in the original fluence simulations. This is because elements such as boron, xenon, silver, gold etc., which have very high thermal neutron capture cross sections, had not been included.

2. High energy inelastic interactions, or spallation. Unlike neutron interactions, radionuclide production cross sections from spallation are not available for all the target nuclei, and are often scarce for particles such as pions. In this study, hadron interaction models in the Monte Carlo particle transport code FLUKA is used [8]. The results then depend on the quality and coverage of the physics models, in particular: nuclear evaporation, the intranuclear cascade, nuclear fission and nuclear fragmentation. Of these the first three are considered to be well modelled but fragmentation, which is important for the heavier target nuclei, is not included in the code. The general features of residual-nuclei production predicted by FLUKA are in reasonable agreement with experimental data [9], exept for light-nuclei production from heavy targets where fragmentation effects start showing up. Fortunately, the bulk of the target nuclei in SCT modules are in the light to medium mass range.

IV. EVALUATING ACTIVITY

Knowledge of the various radionuclide production rates along with their half-lifes allows the calculation of radioactivities; defined as the number of decays per second. The build-up and decay of activity, for each radionuclide, is given by:

$$A = N\,\phi\,(1 - e^{-\lambda t_i})\,e^{-\lambda t_c} \qquad (1)$$

where t_i and t_c are irradiation and cooling times respectively. N is the number of produced radionuclides per p-p event per module, ϕ is the average number of p-p events per second and λ is the decay constant. In going from radionuclide production per p-p event to activity, it is necessary to make certain assumptions about the p-p event rates. The design luminosity of the *LHC* is 10^{34} cm^{-2} s^{-1},

resulting in a p-p interaction rate of $8 \times 10^8\,\mathrm{s}^{-1}$ as predicted by PHOJET [10]. However, the average luminosity over longer timescales will be less due to beam-lifetimes etc. and an averaged luminosity value of $5 \times 10^{33}\,\mathrm{cm}^{-2}\,\mathrm{s}^{-1}$ is assumed [11].

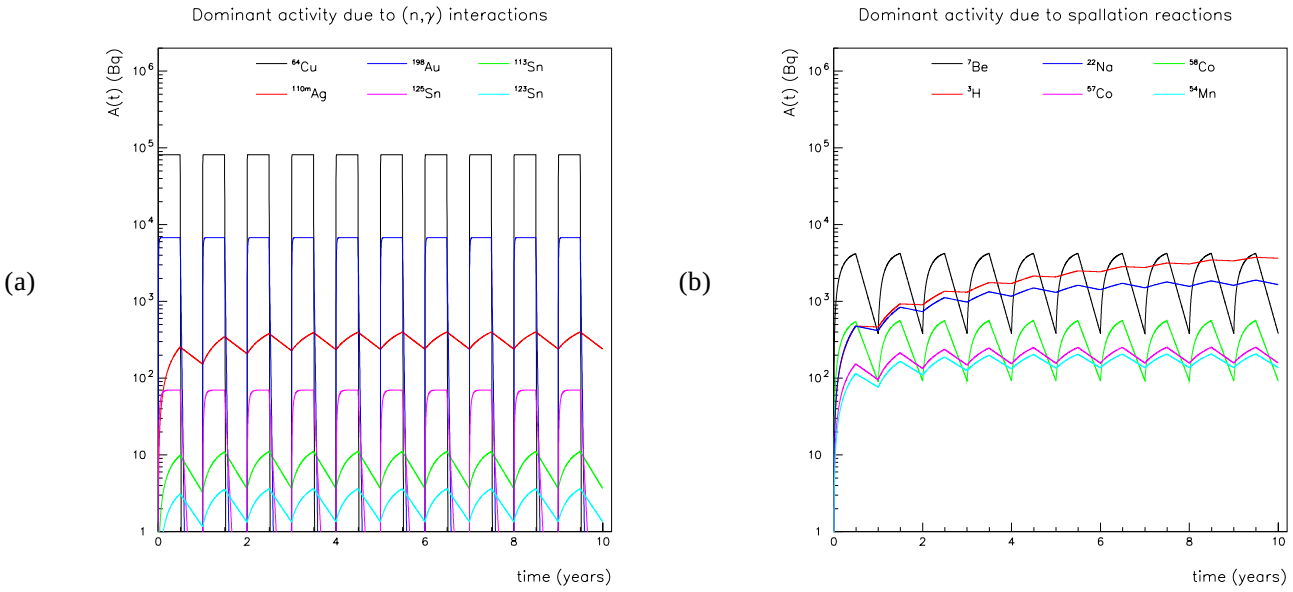

Figure 1: Dominant activities produced by (a) (n,γ) interactions and (b) spallation.

Shown in Figure 1 are the dominant contributions to activation from (n,γ) and spallation reactions. Presented in Table 2 are activities obtained 1 day, 1 week and 1 month after shutdown, for the two cases of one-year of high-luminosity running and ten-years of high luminosity running. A high-luminosity year is defined as 180 days of running (assuming the average beam-luminosity of $5 \times 10^{33}\,\mathrm{cm}^{-2}\,\mathrm{s}^{-1}$) followed by 185 days of shutdown.

V. CALCULATING DOSE RATES

Dose rates are obtained at distances of 10 cm, 30 cm and 100 cm from the centre of a barrel-module. The calculations are facilitated by assuming each module is a point source of radioactivity. This assumption is good for the distances larger than the dimensions of the module (ie 30 cm and 100 cm) and will be conservative by some $\sim$30 % for the value obtained at 10 cm.

A. Dose rates from γ-emitters

The dose rate D_γ from a γ-emitting nuclide can be obtained [12], for a point source, from:

$$D_\gamma = \frac{A.E}{7d^2} \quad \mu Sv/h \tag{2}$$

where A is the activity in MBq, E is the sum of γ energies in MeV weighted by their emission probabilities and d is the distance from the source in metres. The above formula is valid for photons in the range 0.05 to 2 MeV, which is the range covering most of the emitted γs.

Using the activity values given in Table 2 and the relevant gamma decay and energy information, the total gamma dose is obtained by summing the contributions from each radionuclide calculated using equation 2 above. The results are given in Table 3.

B. Dose rates from β-emitters

The dose rate D_β from a β-emitting nuclide can be approximated [12] by:

$$D_\beta = \frac{10\,A}{d^2} \quad \mu Sv/h \tag{3}$$

This expression assumes no absorption of the βs, which can be appreciable depending on the β energy. For example, the average β energy in ^{3}H decay is 5.68 keV. The range in air of such βs is a few mm and will not contribute to external β-doses. However, most of the emitted βs have much higher energies, with ranges in air going up to several metres. In order to avoid overly overestimating the β-doses, the maximum ranges in air of all β-emitters have been obtained and, if the range is shorter than the distance at which the dose is calculated, then it is not included in the total β-dose estimate. The results are given in Table 3.

The above strategy will still overestimate β-doses for two reasons; 1) the ranges are obtained assuming the maximum β-energy and 2) self-shielding of the module material has been neglected. However, the emphasis of the β-dose calculations is to provide reliable upper-limits.

Table 2: Dominant radionuclides contributing to module activity.

Radionuclide	180 days irradiation, cooling times 1day	1week	1month	10 years irradiation, cooling times 1day	1week	1month
^{3}H	477.87	477.43	475.74	3759.17	3755.69	3742.42
^{7}B	4139.23	3828.54	2838.78	4175.48	3862.06	2863.64
^{22}Na	476.32	474.59	466.35	1894.87	1886.59	1855.19
^{24}Na	505.16	0.64	-	505.16	0.64	-
^{31}Si	3.78	-	-	3.78	-	-
^{32}P	13.31	9.95	3.26	13.31	9.95	3.26
^{48}V	45.20	34.97	13.07	45.35	35.01	13.11
^{54}Mn	114.69	113.18	107.55	206.61	203.88	193.74
^{56}Co	106.19	100.73	82.28	110.65	104.96	85.74
^{57}Co	153.14	150.81	142.19	252.27	248.43	234.23
^{58}Co	541.38	510.49	407.57	557.01	525.23	419.33
^{59}Fe	51.79	47.17	32.97	51.97	47.33	33.08
^{60}Co	14.24	14.21	14.09	84.72	84.54	83.85
^{64}Cu	22114.09	8.54	-	22114.09	8.54	-
^{110m}Ag	253.97	249.78	234.35	398.90	392.32	368.07
^{113}Sn	9.81	9.64	8.24	11.04	10.65	9.27
^{123}Sn	3.10	3.01	2.66	3.61	3.50	3.09
^{125}Sn	65.14	42.32	8.09	65.14	42.32	8.09
^{198}Au	5260.37	1127.36	3.07	5260.37	1127.36	3.07

C. Dose rates from Bremsstrahlung

While most of the energy of electrons or positrons is lost through ionisation, there will also be some bremsstrahlung, depending on the energy of the particle and the atomic number Z of the absorbing medium. According to [13], the total bremsstrahlung dose rate from a point source is given by the equation:

$$6 \times 10^{-4} \, \frac{A \, E_m^2}{d^2} \, (Z + I) \, \chi \quad \mu Sv/h \qquad (4)$$

where A and d are as before, E_m^2 is the maximum β energy in MeV, I takes into account *internal bremsstrahlung* and χ is the mass energy absorption coefficient of x-rays in cm^2 g^{-1}. Assuming values of 7, 5 and 0.03 for Z, I and χ respectively [13] for bremsstrahlung in air, it can be seen that equation 4 remains several orders of magnitude lower than equation 4 for all distances and energies. Dose rates from bremsstrahlung can therefore be neglected.

D. Total dose rates for whole barrel system

It is also of interest to estimate dose rates for the entire SCT barrel system. This has been done assuming every module in the barrel system is a point source of identical activation. While this assumption is reasonable for the (n,γ) activation, it will overestimate spallation related dose rates as the relevant particle rates are higher in the first SCT barrel than in the other three barrels. Two 'access scenarios' are considered, shown in Figure 2; the corresponding results are given in Tables 4 and 5.

Table 3: Total γ (β) dose rates (μSv / h) resulting from the activation of a single barrel module.

Distance from the source	180 days irradiating, cooling times 1day	1week	1month	10 years irradiating, cooling times 1day	1week	1month
10 cm	0.161 (28.1)	0.049 (1.3)	0.037 (0.13)	0.215 (28.4)	0.102 (1.4)	0.089 (0.24)
30 cm	0.018 (3.1)	0.005 (0.15)	0.004 (0.015)	0.024 (3.3)	0.011 (0.16)	0.010 (0.027)
1 m	1.61×10^{-3} (0.28)	0.49×10^{-3} (0.013)	0.37×10^{-3} (0.001)	2.15×10^{-3} (0.28)	1.02×10^{-3} (0.013)	0.89×10^{-3} (0.001)

VI. CONCLUSIONS

Concerning (n,γ) activation the dominant radionuclides are ^{64}Cu, ^{198}Au and ^{110m}Ag (see Figure 1). However, ^{64}Cu and ^{198}Au have half-lifes of 12.7 hours and 2.7 days respectively. Therefore, assuming access cannot be made to the SCT within 1 week of shutdown, module activity will be dominated by the ^{110m}Ag which has a half-life of 249.9 days. Considering the small amount of silver as-

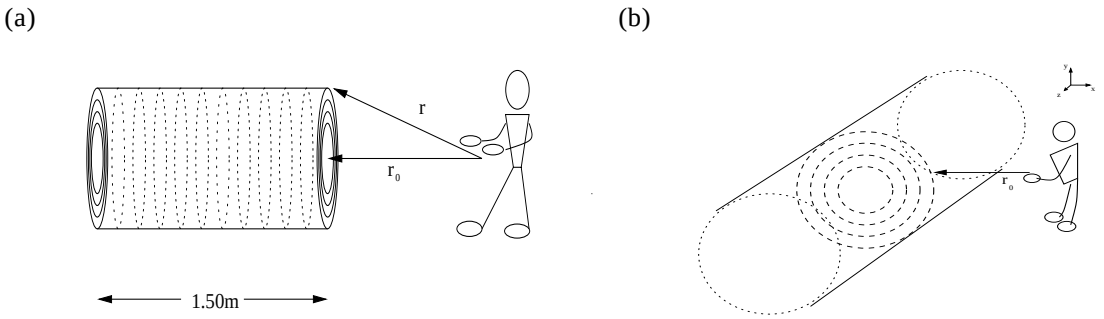

Figure 2: Considered access scenarios (a) Scenario 1 and (b) Scenario 2.

sumed in the module construction (~ 1 mg), it is clear that a design using a higher silver content will result in a proportional increase in activities.

Concerning spallation induced activation, the dominant radionuclides are ^{3}H, ^{7}Be and ^{22}Na. However, when considering external dose rates from activation, ^{3}H can be neglected as discussed in Section V.B. Also, ^{7}Be only decays $\sim 10\%$ of the time into gammas, leaving ^{22}Na as the most important radionuclide resulting from spallation. Interestingly, the target nuclei mainly responsible for ^{22}Na production is silicon and is therefore unavoidable.

Inspection of Table 3 shows that even after 10 years of LHC running and at a distance of 10 cm, the module γ-doses will be about $\sim 0.1\,\mu$Sv / h. The corresponding β-doses (Table 3) are much higher but after 1 week drop to about $1\,\mu$Sv / h. According to the CERN radiation safety manual [14], dose rates less than $0.1\,\mu$Sv / h at 10 cm are considered non-radioactive, while dose rates above $0.1\,\mu$Sv / h but less than $10\,\mu$Sv / h at 10 cm are considered slightly-radioactive. These low dose rates mean that if extraction were necessary then modules could be stored simply in *supervised* areas [14]. After a cool down period of one month, γ-dose and β-dose values of $\sim 0.1\,\mu$Sv / h and $0.24\,\mu$Sv / h at 10 cm are given respectively. These values are similar to those of natural background activity.

Inspection of Tables 4 and 5 show that dose rates from the barrel ensemble will approach $10\,\mu$Sv / h at 10 cm after a 1 month cool-down time. As the predicted values are considered upper-limits, if barrel extraction were necessary then it would probably only need be kept in a supervised area. If the dose rates were higher than $10\,\mu$Sv / h but less than $100\,\mu$Sv / h then the barrel ensemble would have to be stored in a 'controlled' area [14].

Finally, it should be stressed that the current study has assumed a low-silver module design. If the silver content is much higher, as would be the case if silver-loaded conductive glues are used, then the results concerning ^{110m}Ag should be scaled accordingly. However, the radiological implications would have to be reevaluated.

Table 4: Maximum γ (β) doses (μSv / h) for Scenario 1.

Approaching point	180 days irradiating, cooling times 1day		1week		1month		10 years irradiating, cooling times 1day		1week		1month	
10 cm	6.2	(1084)	1.9	(50)	1.4	(4.1)	8.3	(1088)	3.9	(53)	3.4	(7.4)
30 cm	4.0	(695)	1.2	(32)	0.92	(2.4)	5.3	(697)	2.5	(34)	2.2	(4.1)
100 cm	1.3	(184)	0.38	(9.5)	0.29	(0.35)	1.7	(184)	0.79	(9.6)	0.69	(0.47)

Table 5: Maximum γ (β) doses (μSv / h) for Scenario 2.

Approaching point	180 days irradiating, cooling times 1day		1week		1month		10 years irradiating, cooling times 1day		1week		1month	
10 cm	9.2	(1598)	2.8	(74)	2.1	(6.4)	12	(1603)	5.8	(79)	5.1	(12)
30 cm	5.1	(888)	1.6	(41)	1.2	(3.4)	6.8	(891)	3.2	(43)	2.8	(5.7)
100 cm	1.5	(254)	0.45	(11)	0.34	(0.48)	1.99	(254)	0.95	(12)	0.83	(0.66)

VII. REFERENCES

[1] I.Dawson, Review of the Radiation Environment in the Inner Detector, ATL-INDET-2000-006

[2] SCT Barrel Module, Final Design Reviews: SCT-BM-FDR-1, SCT-BM-FDR-2, SCT-BM-FDR-3 and SCT-BM-FDR-4. Available from: http://atlasinfo.cern.ch/Atlas/GROUPS/INNER_DETECTOR/SCT/module/SCTbarrelmod.html

[3] Table of material for the Cu/Polyimide hybrid 12 μm Copper, version 4. Available from: http://jsdhp1.kek.jp/~unno/si_hybrid/k4/KhybridXo01feb26.pdf

[4] Private communication, T.Weidberg

[5] T.Niinikoski, Evaporative Cooling - Conceptual Design for ATLAS SCT, ATL-INDET-98-214

[6] Evaluated Nuclear Data Files (ENDF), obtained from: http://www-nds.iaea.org/ndsstart.html

[7] Chart of the Nuclides, produced by Knowles Atomic Power Laboratory; 14th edition - revised to April 1988. (Using National Nuclear Data Center (NNDC) files.)

[8] A.Fasso, A.Ferrari, J.Ranft and P.Sala, Full details can be found at FLUKA official website; http://fluka.web.cern.ch/fluka/

[9] A.Ferrari and P.Sala, The Physics of High Energy Reactions, ATLAS Internal note, PHYS-NO-113, 1997

[10] R.Engel and J.Ranft, *Hadronic photon-photon interactions at high-energies*, Physics. Rev. D54:4244-4262, 1996

[11] K.Potter and G.Stevenson, *Average Interaction Rates for Shielding Specification in High Luminosity LHC Experiments*, CERN AC/95-01, CERN/TIS-RP/IR/95-05.

[12] K.J.Connor and I.S.McLintock, *Radiation Protection*, HHSC Handbook No. 14, 1997, ISBN 0-94237-21-X

[13] I.S.McLintock, *Bremsstrahlung from Radionuclides*, HHSC Handbook No. 15, 1994, ISBN 0-948237-23-6

[14] Radiation Safety Manual, CERN – TIS/RP, 1996